Colloids and Surfaces B: Biointerfaces 81 (2010) 289–296

Contents lists available at ScienceDirect

Colloids and Surfaces B: Biointerfaces

journal homepage: www.elsevier.com/locate/colsurfb

PDMS-based porous particles as support beds for cell immobilization: Bacterial biofilm formation as a function of porosity and polymer composition

M.R. Fernández[a], M.G. Casabona[a], V.N. Anupama[b], B. Krishnakumar[b], G.A. Curutchet[c], D.L. Bernik[a,*]

[a] Instituto de Química Física de Materiales, Ambiente y Energía (INQUIMAE), Departamento de Química Inorgánica, Analítica y Química Física, Facultad de Ciencias Exactas y Naturales, Universidad de Buenos Aires, Argentina
[b] Environmental Technology, National Institute for Interdisciplinary Science & Technology (NIST, CSIR-India), Thiruvananthapuram 695019, India
[c] Escuela de Ciencia y Tecnología, Universidad Nacional de San Martín, San Martín, Provincia de Buenos Aires, Argentina

ARTICLE INFO

Article history:
Received 19 February 2010
Received in revised form 8 July 2010
Accepted 8 July 2010
Available online 10 August 2010

Keywords:
Biofilm
Bed material
CSLM
SEM
PDMS

ABSTRACT

The objective of this work is to test the performance of new synthetic polydimethylsiloxane (PDMS)-based bed particles acting as carriers for bacteria biofilms. The particles obtained have a highly interconnected porous structure which offers a large surface adsorption area to the bacteria. In addition, PDMS materials can be cross-linked by copolymerization with other polymers. In the present work we have chosen two hydrophilic polymers: xanthan gum polysaccharide and tetraethoxysilane (TEOS). This versatile composition helps to modulate the interfacial hydrophobic/hydrophilic balance at the particle surface level and the roughness topology and pore size distribution, as revealed by scanning electron microscopy. Biofilm formation of a consortium isolated from a tannery effluent enriched in *Sulphate Reducing Bacteria* (*SRB*), and pure *Acidithiobacillus ferrooxidans* (*AF*) strains were assayed in three different bed particles synthesized with pure PDMS, PDMS–xanthan gum and PDMS–TEOS hybrids. Bacterial viability assays using confocal laser scanning fluorescence microscopy indicate that inclusion of hydrophilic groups on particle's surface significantly improves both cell adhesion and viability.

1. Introduction

Microorganisms are regularly used to degrade pollutants in order to minimize contamination caused by industrial activities. In many cases bioremediation processes are performed using bioreactors, where the extensive prior experience indicates that in most cases the immobilization of microorganisms on beds improves biocatalysis (Michel et al. [1]; Wang et al. [2]; Strathmann et al. [3]).

The objective of this work is to obtain bed particles designed to be used in lab scale reactors or in water reservoirs within the frame of a project devoted to chromium VI bioremediation. Leather is a typical Argentine export and in consequence tanneries proliferate at the suburbs of Buenos Aires City. Therefore we wanted to know if a consortium of bacteria taken from a tannery effluent was able to adhere and grow in PDMS-based particles, and optimize the design of the particles to improve cell growth. For that reason we have selected a single bacterial strain capable of participating in a process for bioremediation of chromium VI. Thus, a single strain can work under controlled conditions to study the influence of polymer composition on biofilm formation and cell viability.

Immobilization and biofilm formation are natural processes when bacteria grow and reproduce in presence of the appropriated surfaces, exhibiting differential phenotypic characteristics with respect to their planktonic counterparts (Donlan and Costerton [4]). As highlighted by many authors, attachment of cells to a surface is a complex process that is influenced by the diverse characteristics of the substratum, bacterial cell surface, the adhesive molecules secreted by the microorganisms and the growth medium, allowing alterations in the thickness and spreading of the biofilm on the carrier surface (Krishnan et al. [5]; Tirrell et al. [6]; Yun et al. [7]). Microbial immobilization appears to increase as the surface roughness increases, because shear forces are diminished, and more substratum surface area is available for adsorption (Pasmore et al. [8]; Wagner et al. [9]). Besides, the bacterial cell surface characteristics such as hydrophobicity, extracellular polymeric substances production and the presence of *fimbria* and *flagella* will influence the rate and extent of attachment (Zita and Hermansson [10]; Donlan [11]).

The surface hydrophobicity of the substratum also plays an important role in bacterial adhesion. Many researchers have reported that microorganisms adhere more efficiently to hydrophobic materials than to hydrophilic ones (Hood and Zottola [12]; Parkar et al. [13]; Pasmore et al. [8]). However, the influence of the surface hydrophobicity is still controversial. In contrast with the hypothesis that hydrophobic surfaces promote the adhesion of

* Corresponding author at: INQUIMAE: Ciudad Universitaria, Pabellón 2, C1428GHA Buenos Aires, Argentina. Tel.: +54 11 45763358; fax: +54 11 45763341.
E-mail address: dbernik@qi.fcen.uba.ar (D.L. Bernik).

0927-7765/$ – see front matter © 2010 Elsevier B.V. All rights reserved.
doi:10.1016/j.colsurfb.2010.07.018

bacteria, Chavant et al. [14] and Lackner et al. [15] reported that the biofilm formation was faster on hydrophilic surfaces. Krishnan et al. [16] described the anti-biofouling properties of surfaces containing amphiphilic side chains which influence the adhesion of microorganisms. Sohn et al. [17] reported that bacterial adherence after 24 h was much lower when using a non-polar surface (poly(oxyethylene) derivatives) in comparison with normal PDMS. Satriano et al. [18] found that the presence of hydrophilic SiO_2-like holes within hydrophobic polyhydroxymethylsiloxane (PHMS) favours bacterial cell attachment with respect to the pure PHMS non-polar surface, and Bertin et al. [19] reported that an aerobic coculture had better performance on the bioremediation of organic pollutants when adsorbed onto silica beds than when fixed on non-polar polyurethane foams. These last reports in particular suggest that the presence of hydroxyl groups favours bacterial cell attachment. With this in mind, we synthesized three different porous bed particles based on PDMS polymer, two of them bearing hydroxyl groups introduced by doping PDMS with hydrophilic xanthan gum and with TEOS (tetraethylorthosilicate), respectively. Topology and pore morphology of the three different materials were analysed by SEM and bacterial adhesion and cell viability were assayed by using commercial DNA staining fluorescence kits and confocal laser scanning microscopy.

2. Materials and methods

2.1. Chemicals

Polydimethylsiloxane (PDMS, Sylgard 160) was provided by Dow Corning (USA). Tetraethylorthosilicate (TEOS, 99.999%) was purchased from Fluka. Xantham gum was provided by Fisher Scientific (Pittsburgh, PA). The fluorescent probes for bacterial staining SYBR Green I and LIVE/DEAD® BacLight™ Bacterial Viability Kits were provided by Invitrogen (Catalog No. 13152e, Molecular Probes). Potassium permanganate, ammonium sulphate, potassium chloride, potassium phosphate dibasic anhydrous, manganese sulphate heptahydrate, calcium chloride, ferrous sulphate hexahydrate, sulphuric acid and sodium azide were all purchased by sigma, analytical grade and used as received.

2.2. Bacterial strains and media

The first adsorption assay was done with a consortium isolated from a tannery effluent enriched in *Sulphate Reducing Bacteria* (SRB), belonging to the culture collection of the Environmental Technology Division (NIST, CSIR-India).

Acidithiobacillus ferrooxidans (strain DSM 11477) was provided by one of the authors (G. Curutchet, UNSAM), and was cultured in 9K medium containing (in g/L): 2.0 $(NH_4)_2SO_4$, 0.1 KCl, 0.5 K_2HPO_4, 0.5 $MgSO_4{\cdot}7H_2O$, 0.01 $CaCl_2$ and 44 $FeSO_4{\cdot}6H_2O$. The culture pH was adjusted to 1.8 with H_2SO_4. *A. ferrooxidans* was sub-cultured once, 10% (v/v), before inoculation for experiments at 30 °C and 50 rpm until cell content was 10^8 approximately.

2.3. Bed synthesis

Three different types of PDMS bed particles were synthesized: pure PDMS, PDMS–xanthan gum (99–1%, w/w) and PDMS–TEOS (80–20%, w/w) hybrids were obtained by mixing pure PDMS and the corresponding copolymers with a mechanical stirrer (2000 rpm) before curing. The mixture was slightly diluted with heptane (the natural PDMS's solvent) in order to decrease viscosity and favour mechanical mixing. After mixing thoroughly for 10 min, the curing was accomplished dropping drop by drop in distilled water at 75 °C. After 5 min the temperature was increased until 80 °C for 5 more minutes. Particles were collected and dried under high vacuum at room temperature. This process allows the obtaining of bed particles of about 3 mm diameter with the aspect of porous lentils.

2.4. Baclight live/dead bacterial viability kit

The LIVE/DEAD® BacLight™ Bacterial Viability Kit utilizes a mixture of SYTO 9 green-fluorescent nucleic acid stain and the red-fluorescent nucleic acid stain, propidium iodide (PI). These stains differ both in their spectral characteristics and in their ability to penetrate healthy bacterial cells. When used alone, the SYTO 9 stain generally labels all bacteria in a population, those with intact membranes and those with damaged membranes.

In contrast, propidium iodide penetrates only bacteria with damaged membranes, causing a reduction in the SYTO 9 stain fluorescence when both dyes are present. Thus, with an appropriate mixture of the SYTO 9 and propidium iodide stains, bacteria with intact cell membranes stain fluorescent green, whereas bacteria with damaged membranes stain fluorescent red.

2.5. Biofilm preparation and fluorescence staining

The SRB enriched culture was incubated with pure PDMS particles for three days at 30 °C. Particles were gently washed before staining with SYBR Green I. After incubation during 30 min, they were observed with 50× magnification with an epifluorescent microscope Leica DM 2500, equipped with a digital camera DFC300FX.

Three equal aliquots from the same batch culture of *A. ferrooxidans* in exponential growth were added to different 250 ml Erlenmeyer flasks containing 1 g of each bed type. Samples were incubated at 30 °C gently shaked at 50 rpm for two days to allow cell attachment. During the experiment, bacterial activity was monitored by measuring ferrous iron concentration by titration with potassium permanganate 0.01N and the pH was measured with a glass electrode periodically. After 24 h of incubation bed particles were removed from each culture, and washed once with Milli-Q water to remove grown media to avoid possible interferences prior staining. Each particle of a volume of approximately 0.01–0.02 cm^3 was stained with 300 μl of LIVE/DEAD BacLight viability kit prepared according to the manufacturer's instructions and samples were incubated in the dark at room temperature for 15 min. The final concentration of PI is 30 μM and SYTO 9 was 6 μM. Several control assays were run to ensure that the observed staining is not due to non-specific material's or probe's fluorescence. Controls related to bed's own fluorescence and non-specific staining of the beds with each fluorescent stain were done; no fluorescence was detected in any case (beds were treated with 0.1 mM sodium azide and UV light for 15 min before the addition of the staining solution). The same negative result was obtained when checking out cell's and fresh medium's autofluorescence. Interference between each fluorescent dye for bacteria staining were tested using biofilms supported on the carriers with only one fluorescent stain at a time and then using both simultaneously, obtaining fluorescence just when using the right fluorophore in combination with the right laser. Additionally, appropriate detection of damaged cells was confirmed by exposing carriers with biofilms on their surfaces to UV light for 30 min before incubation with the staining solutions.

2.6. Visualisation method and picture processing

Examination was done using a confocal laser scanning fluorescence microscope (CLSM, OLYMPUS FV300/BX61) using sequential Blue Argon (488 nm) and Green Helium Neon (543 nm) excitation lasers and cut off emission filters of 510–530 and 575–615 respectively. This combination avoids any possibility of overlapping

between probes. OLYMPUS FLUOVIEW FV1000 Ver.1.6a Viewer was used for the analysis of the pictures obtained by the OLYMPUS FV300/BX61 microscope, this software allowed us to make an integration of the images of each cut to obtain a complete vision of the surface of our three porous particles with a *A. ferrooxidans* biofilm on the their surfaces as well as an analysis of the successive cuts that made the complete picture to determine the thickness of the biofilm in each place of the particle's surface. OLYMPUS FLUOVIEW FV1000 Ver.1.6a Viewer was also used to estimate pore size distribution in the SEM images.

3. Results

As an assay to test the feasability of pure silicone particles (PDMS) as porous beds for biofilm formation, a mixed culture enriched in SRB was used. After three days of incubation, the staining with the DNA marker SYBR Green I resulted in the fluorescent pattern shown in Fig. 1. The pictures show the high degree of porosity and surface roughness of the material, with many pores with diameters ranging from several tenths of microns (200–400 μm) for the largest pores up to only few microns for the smallest. On these pictures given the characteristics of the microscope used it was a priority to focus inside the pore cavities where many small green-fluorescent patches can be visualized. Since SYBR Green I is a DNA-intercalating dye and the non-specific fluorescence controls were negative, the green fluorescence patches are attributed to incipient bacterial biofilm formation.

This first assay prompted us to study other PDMS-based polymers, focusing on the influence of pore size and surface polarity changing the hydrophobic/hydrophilic balance by the incorporation of more hydrophilic molecules. In this regard, we decided to study the adhesion of a single bacteria strain (*A. ferroxidans*) in order to center the attention on the effect produced by the differences in chemical composition and surface topology between pure PDMS and the hybrids PDMS–xanthan gum and PDMS–TEOS.

Xanthan gum is a natural polysaccharide produced by fermentation of glucose by *Xanthomonas campestres*. It is an anionic polyelectrolyte with a β-(1 → 4)-D-glucopyranose glucan backbone with side chains of mannopyranose-glucuronic acid-mannopyranose on alternating residues Mundargi et al. [20]. It hydrates rapidly in cold water yielding viscous solutions acting as a stabilizer and emulsifying agent, being relatively unaffected by ionic strength, pH (1–13), shear or temperature Mandala and Bayas [21]. On the other hand TEOS (tetraethylorthosilicate) is a chemical precursor for sol–gel polycondensation reactions which give place to the synthesis of silicon aerogels. The presence of numerous hydroxide groups in both copolymers allow these molecules to cross-link with PDMS along the curing process of bed synthesis.

Although PDMS and the two PDMS hybrids were synthesized by matching procedures, the topology of the particles obtained was significantly different both in the number of pores as pore size distribution. This can be clearly visualized in the electron scanning microscopy (SEM) pictures of Fig. 2. SEM pictures show that pure PDMS particles have relatively few pores, which are wider in comparison to the ones in PDMS–xanthan, and this in turn has fewer and larger pores than PDMS–TEOS.

Pore size analysis showed that the higher pore diameter average was achieved by particles made of PDMS (252.18 ± 248.27) ($n = 60$) followed by the ones made of PDMS–Xanthan gum (135.95 ± 79.79) ($n = 147$), and ending with the particles composed by PDMS–TEOS (92.43 ± 47.56) ($n = 388$), where "n" in this case is the total amount of pores in the respective particle image obtained by SEM showed in Fig. 2. Additionally, the presence of not visible pores in the SEM images (in the order of the micrometer) and therefore not included in pore size analysis, can be visualized in the CLSM images

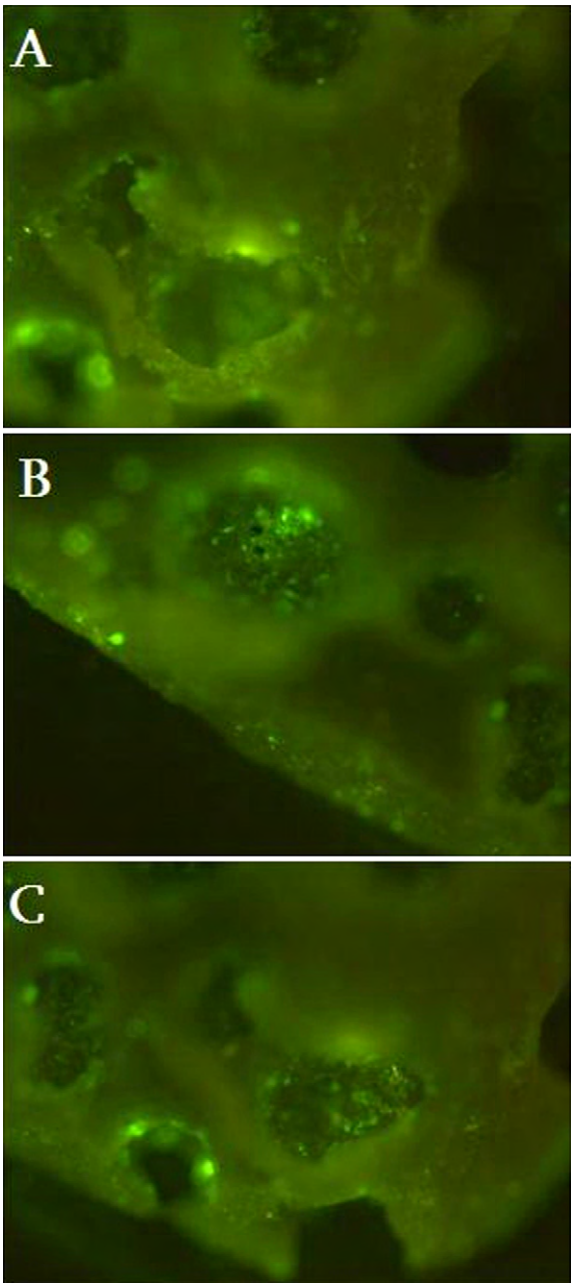

Fig. 1. Fluorescence staining of an enriched *SRB* bacteria culture adsorbed on pure PDMS bed particles with the DNA-intercalating probe SYBR Green I. The three pictures show a very rough surface and deep holes in the particle structure, and the bacteria adhered mainly in the pore borders and inside the cavities.

because of the fluorescence surrounding them due to bacterial growth around these small pores.

The evident differences between the topology of the three synthesized bed supports allowed us to study the influence of bed surface polarity (with different chemical groups exposed) and the whole pore size distribution on biofilm formation. Thus, we incubated each type of bed particles with *A. ferrooxidans* culture as described in Section 2. In this case, the fluorescent kit used was the LIVE/DEAD® BacLight™ Bacterial Viability Kit, which differentiates cells with damaged/intact membrane which in most cases is correlated with cell viability. In addition, observations were done with a confocal laser scanning fluorescence microscope, allowing us to see the rough surface of bed particles and the biofilm in detail. Pictures shown in Fig. 3 point out remarkable differences in biofilm

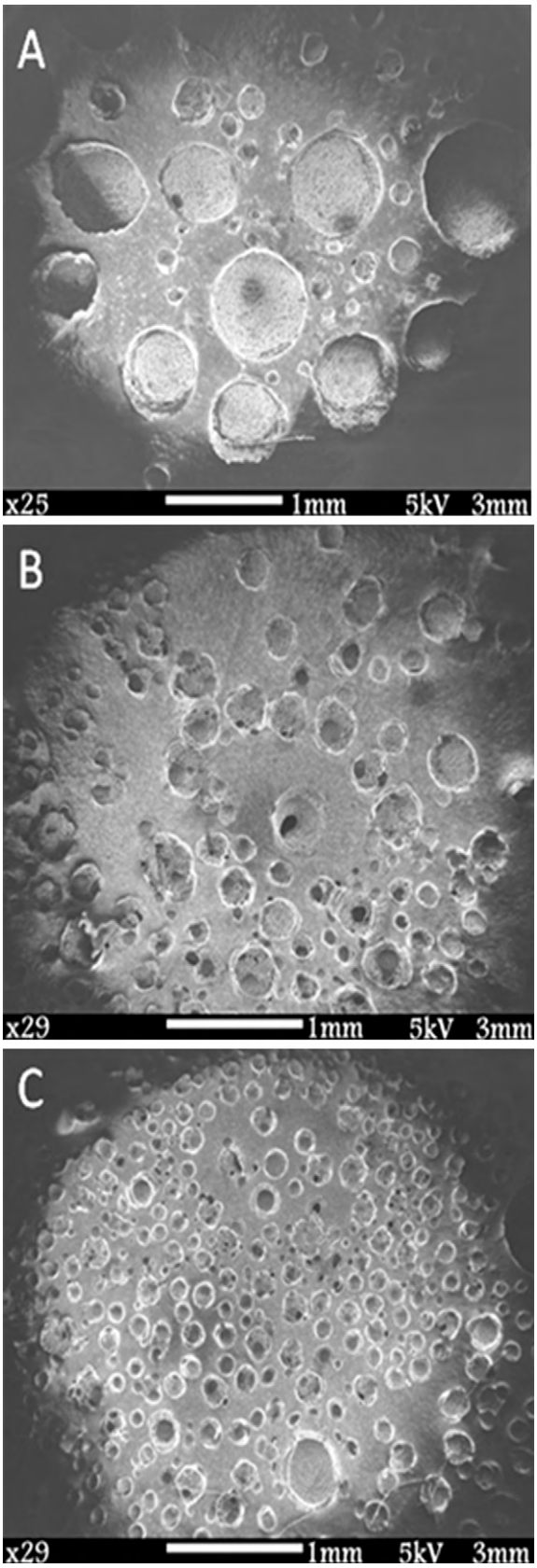

Fig. 2. SEM images of the three types of polymer particles synthesized. Pictures are taken with very similar magnification in order to compare the relative pore size distribution. A: pure PDMS, B: PDMS–xanthan gum hybrid, and C: PDMS–TEOS hybrid.

features in the three different types of beds. The green fluorescence stains the viable cells whereas the red fluorescence indicates dead cells. Comparing Fig. 3A–C, it is evident that the hybrid PDMS–TEOS particles have the strongest green fluorescence while pure PDMS particles have the strongest red one accompanied by the weakest green fluorescence.

It is worth to mention that the intensity of the SYTO9 fluorescence (which is the green component of the viability kit) is independent of the intensity of red fluorescence of propidium iodide (the red component of the kit) because illumination in the CLS microscope was accomplished by two independent excitation lasers: Blue Argon (488 nm) and Green Helium Neon (543 nm). The red and green fluorescence shown in Fig. 3 represent the integration of the total number of planes swept by the microscope along the scanning: the microscope was set up to scan and register the digital image of different planes from the bulk to the carrier's surface each 5 μm. Thus, the results obtained with the viability kit show a clearly higher total green fluorescence for the two PDMS hybrids, in particular for the PDMS–TEOS material.

In addition, the plane by plane analysis of the relative green and red fluorescence intensity gives information about the particular features of the material that may influence the formation of the biofilm and the relative proportion of dead and alive cells. In this regard, in Fig. 4 it is possible to see different cuts of the biofilms on the pure PDMS support chosen so as to highlight a selected area of the biofilm, showing that the most intense red-fluorescent areas are surrounding the biggest pores of the material. Analysing the sequence of planes taken by the microscope it is observed that pores that protrude from the surface generate immediate deep concavities around them, just where the strongest red fluorescence intensity is located. In the red area in Fig. 4 the height of the developed biofilm is approximately 50 μm (see the boxes) beginning in Fig. 4C and ending in L (10 successive planes, each one of 5 nm height).

In order to make a more valuable statistical estimation of biofilm thickness, several fluorescent spots in each picture were analysed, quantified by the parameter "*n*". In this case "*n*" represents the number of fluorescent spots analysed in each picture in order to estimate the film thickness. That is if "*n*" is 30, this means that 30 different fluorescent patches in the picture were analysed plane by plane in order to see when the fluorescence starts and when it ends. Since each plane is separated from the next by 5 nm, the total number of fluorescent planes yields an estimation of the biofilm thickness in that fluorescent patch, and the mean thickness obtained with the n number of patches is the reported value.

In Fig. 5 we compared the height of the *A. ferrooxidans* viable biofilms on the three different carriers, pure PDMS, PDMS–xanthan gum and PDMS–TEOS after 24 h of incubation, stained using LIVE/DEAD® BacLight™ Bacterial Viability Kit. The methodology followed is similar to that used in Fig. 4: an area is selected in the image and successive planes are analysed to detect incipient and vanishing fluorescence. The white rectangles in picture A1, B1 and C1 delimit the amplified region showed in figures A2–A5, B2–B5 and C2–C5 for PDMS, PDMS–xanthan gum and PDMS–TEOS, respectively. Figures A2–A5 show 4 successive cuts of the biofilm on PDMS particles, A2 is the cut just before a clear visualization of fluorescence into the white square, A3 and A4 represent two intermediate cuts where fluorescence is present and A5 is the first cut just after fluorescence disappears. Whereas figures B2–B5 and figures C2–C5 show a similar sequence of the biofilm described before, but on PDMS–xanthan gum and PDMS–TEOS, respectively. For PDMS–xanthan gum and PDMS–TEOS particles only two intermediate cuts were showed for practical reasons. These pictures are representative of the biofilm observed all over each type of surface.

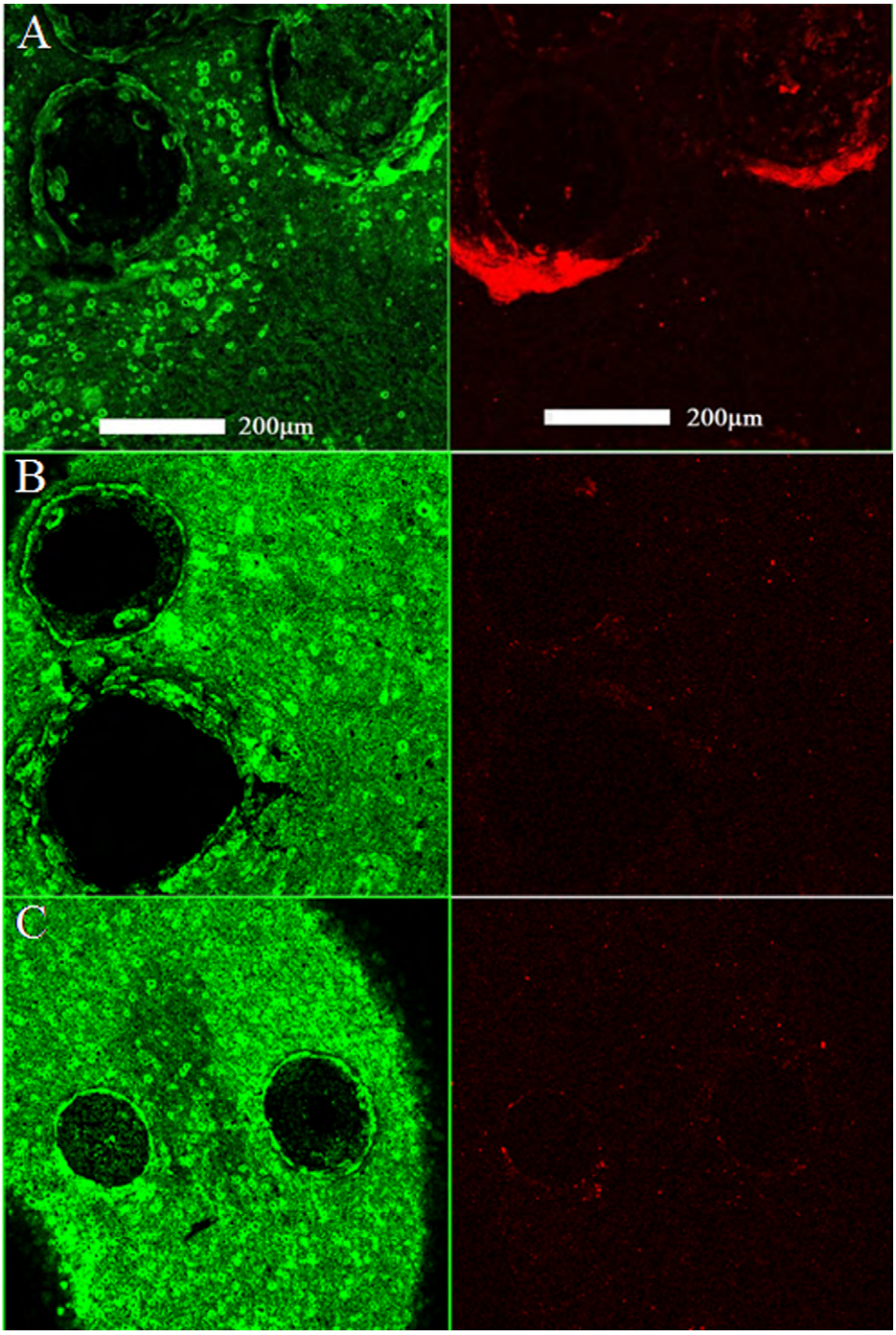

Fig. 3. Confocal laser scanning fluorescence microscopy of the three types of bed supports after 24 h of incubation with *A. ferrooxidans*. Fluorescent staining was achieved using LIVE/DEAD BacLight viability kit (Invitrogen, see Section 2). Green and red patches stain viable and dead cells, respectively. (A) PDMS, (B) PDMS–xanthan gum, and (C) PDMS–TEOS. (For interpretation of the references to color in this figure caption, the reader is referred to the web version of the article.)

Interestingly, in flat areas (see Fig. 5A1–A5) the biofilm fluorescing in green obtained with the pure PDMS carrier is much thinner than the biofilm fluorescing in red: $11 \pm 3\,\mu m$ ($n = 30$) (Fig. 5A3–A4) and $50 \pm 14\,\mu m$ ($n = 15$) (Fig. 4) depth, respectively. Additionally, the biofilm produced on PDMS–Xanthan gum was $23 \pm 7\,\mu m$ ($n = 30$) and on PDMS–TEOS it was $27 \pm 7\,\mu m$ ($n = 30$). When analysing if there is a significant difference between the mean height values of the biofilms on the three different surfaces it was observed that films obtained for PDMS was significantly shorter than the one found for PDMS–xantham gum and PDMS–TEOS (p-value < 0.01 in both cases), whereas the comparison between PDMS–xantham gum with PDMS–TEOS yielded means which were significantly different with a p-value < 0.05.

4. Discussion

Poly(dimethylsiloxane) (PDMS) is a flexible, versatile, biocompatible and inexpensive polymer. The surface properties of PDMS often demand further modifications for its successful application in biotechnology, due to its hydrophobic characteristics and non-

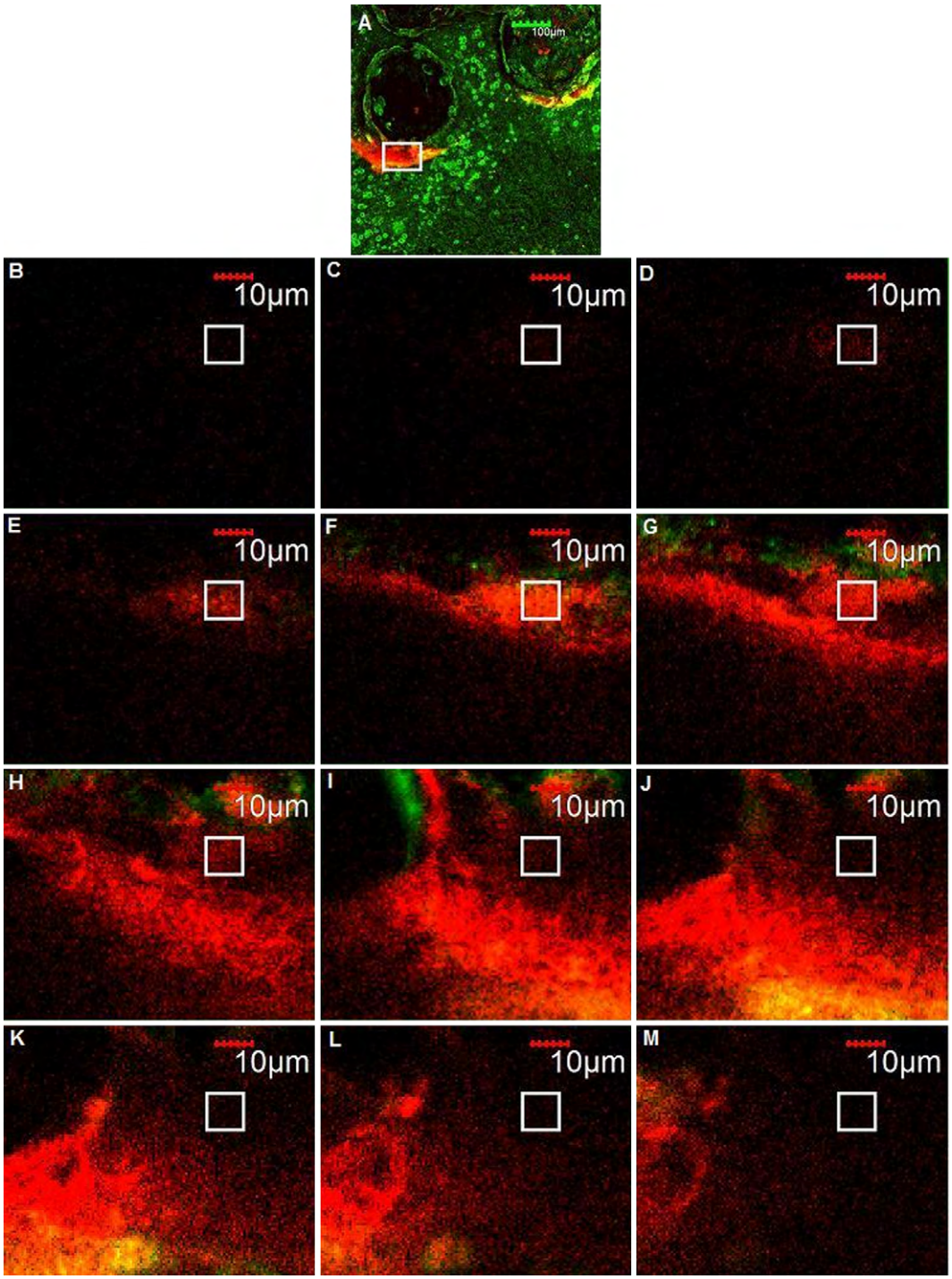

Fig. 4. Biofilm height analysis of the non-viable cell regions of *A. ferroxidans* biofilm on pure PDMS bed. The square in (A) shows the amplified region to be analysed. The following pictures from B to M show successive planes of the biofilm in the afore depicted square in *A*, to see along how many planes the fluorescence persist. Red fluorescence is perceivable into the squares from picture (C) to (L), which give a total height of 50 nm. See text for more details. (For interpretation of the references to color in this figure caption, the reader is referred to the web version of the article.)

specific protein adsorption. Various methods have been utilized to obtain a hydrophilic PDMS surface (Makamba et al. [22]; Liu and Lee [23]; Vilkner et al. [24]), including oxygen plasma (Duffy et al. [25]), UV/ozone (Xiao et al. [26]), silanization (Sui et al. [27]; Hellmich [28]; Delamarche et al. [29]), radiation-induced graft polymerization (Barbier et al. [30]; He et al. [31]) and photoinduced graft polymerization (Hu et al. [32]; Hu et al. [33]).

Although in some applications PDMS porosity can be considered a disadvantage (Shin et al. [34]), we regard this property as beneficial and we enhance it by introducing additional chemical groups by building polymer hybrids thus modifying its surface polarity and topography.

In this work, the copolymerization of PDMS with more hydrophilic polymers such as TEOS and Xanthan gum allows to see the influence of the increasing polarity on bacterial adhesion. In addition, the highly porous particles obtained have two main advantages in the perspectives of the present work: one is that high porosity makes the material suitable for encapsulation pur-

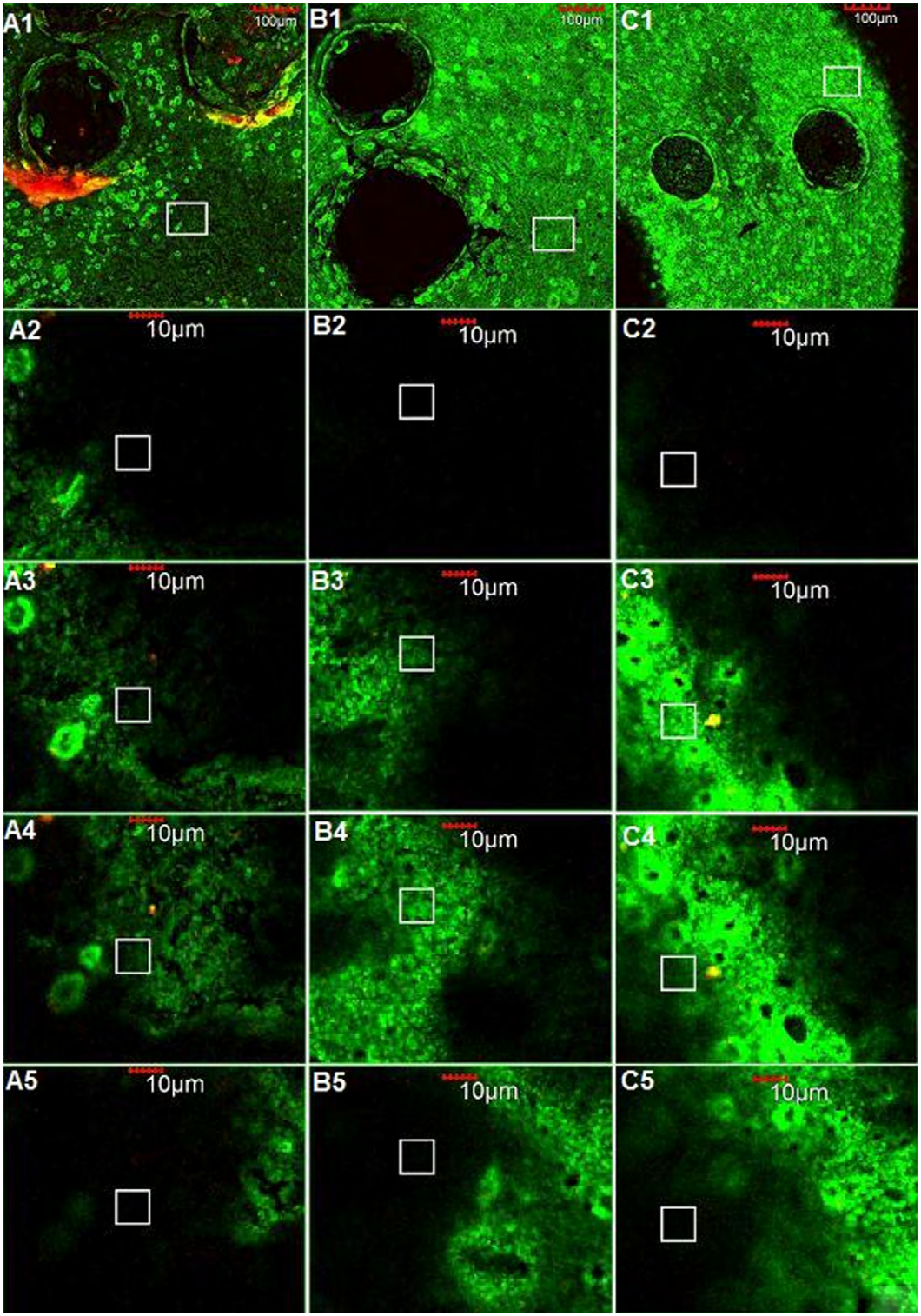

Fig. 5. Comparison of the biofilm height on the three different carriers after 24 h of incubation. Series of images A, B and C belongs to pure PDMS, PDMS–xanthan gum and PDMS–TEOS, respectively, with a biofilm of *A. ferrooxidans* on each surface stained using LIVE/DEAD® BacLight™ Bacterial Viability Kit. The white rectangles in picture A1, B1 and C1 delimit the amplified region showed in successive figures A2–A5, B2–B5 and C2–C5. The onset and end of the green fluorescence allow the calculation of film height. For more details see text in Section 3. (For interpretation of the references to color in this figure caption, the reader is referred to the web version of the article.)

poses and second is that it is well known that roughness favours bacterial adhesion due to both major surface area available and also because rough surfaces provide more shielding from shear forces (Pederson [35]).

From the results it is clear that the pure PDMS bed particles show the lowest cell adhesion and viability. This result is supported by numerous previous reports demonstrating that pure PDMS has good fouling release properties (Krishnan et al. [5] and [16]). In addition, Figs. 1 and 3 shows that the bigger amount of viable cells is preferentially adhered around the pores on the material surface. This might be due to the fact that these are the regions where less shear stress is produced when shaking the samples dur-

ing bacterial cultures (Pederson [35]). If this is so, bacteria start growing first there; but, if the cavity around the hole is too deep, diffusional problems appear as a consequence of the increasing film thickness, limiting the nutrient accesses and the release of toxic by-products from bacterial metabolism, ultimately causing cell death (red spots when staining). On the contrary, in the proximity to smaller pores there are less deep concavities so biofilms are shorter in height, thus having less diffusional problems and resulting in higher bacterial viability (Chang et al. [36]; Hunt et al. [37]).

The porosity of the obtained beds is extensive and some holes traverse the particles (pictures not shown). However, the former analysis regarding the observations made in Fig. 4 suggests that at deep cavities bacterial survival will be difficult due to diffusional restrictions. Nonetheless, the high internal porosity gives to the material the lower density needed to move easily in the liquid of an air-lift reactor, a fact which we infer will optimize mixing along bioremediation process.

The analysis of the results shown in Figs. 1 and 3 indicates that the availability of more adsorption sites at the bed's surface improves biofilm formation. In addition, the analysis of Figs. 4 and 5 points out that the presence of greater number of adsorption sites around pores of smaller height enhances cell viability. In both cases, from the three different polymers assayed, PDMS–TEOS hybrid shows the best performance.

5. Conclusions

The copolymerization of PDMS with polyhydroxylated polymers such as xanthan gum and TEOS results in obtaining bed particles which offer more suitable surfaces for bacterial biofilm development and viability of *A. ferrooxidans*. In particular, we conclude that the PDMS–TEOS is, within the three materials assayed herein, the most appropriate bed support to develop *A. ferrooxidans* biofilms under the culture conditions tested. Future studies will be directed to ascertain the performance of the biofilms under different stress conditions such as differential nutrient supplies, pH, temperature and shear stress in air-lift bioreactors.

Acknowledgements

We thank Dr. Claudia Marchi and Dr. Roberto Fernández (University of Buenos Aires) for their invaluable help on the SEM and CLSM techniques, respectively. DLB and GAC are research members of the *Carrera del Investigador Científico* (CONICET, Argentina). Financial support was received from CONICET (PIP 112-200801-01210), University of Buenos Aires (UBACyT 2008-2010, project X157) and Agencia Nacional de Promoción Científica y Tecnológica (PICT 2006-00568).

References

[1] C. Michel, M. Jean, S. Coulon, M.C. Dictor, F. Delorm, D. Morin, F. Garrido, Appl. Microbiol. Biotechnol. 77 (2007) 457–467.
[2] Y. Wang, Y. Fan, Ji-Dong Gu, Int. Biodeterior. Biodegr. 53 (2004) 93–101.
[3] M. Strathmann, T. Griebe, H.C. Fleming, Appl. Microbiol. Biotechnol. 54 (2000) 231–237.
[4] R.M. Donlan, J.W. Costerton, Clin. Microbiol. Rev. 15 (2002) 167–193.
[5] S. Krishnan, C.J. Weinman, C.K. Ober, J. Mater. Chem. 18 (2008) 3405–3413.
[6] M. Tirrell, E. Kokkoli, M. Biesalski, Surf. Sci. 500 (2002) 61–83.
[7] M. Yun, K. Yeon, J.S. Park, C.H. Lee, J. Chun, D.J. Lim, Water Res. 40 (2006) 45–52.
[8] M. Pasmore, P.W. Todd, B. Pfiefer, M. Rhodes, C.N. Bowman, Biofouling 18 (2002) 65–71.
[9] M. Wagner, N.P. Ivleva, C. Haisch, R. Niessner, H. Horn, Water Res. 43 (2009) 63–76.
[10] A. Zita, M. Hermansson, Appl. Environ. Microbiol. 63 (1997) 1168–1170.
[11] R.M. Donlan, Emerg. Infect. Dis. 8 (2002) 881–890.
[12] S.K. Hood, E.A. Zottola, Food Control 6 (1995) 9–18.
[13] S.G. Parkar, S.H. Flint, J.S. Palmer, J.D. Brooks, J. Appl. Microbiol. 90 (2001) 901–908.
[14] P. Chavant, B. Martinie, T. Meylheuc, M.N. Bellon-Fontaine, M. Hebraud, Appl. Environ. Microbiol. 68 (2002) 728–737.
[15] S. Lackner, M. Holmberg, A. Terada, P. Kingshott, B.F. Smets, Water Res. 43 (2009) 3469–3478.
[16] S. Krishnan, R. Ayothi, A. Hexemer, J.A. Finlay, K.E. Sohn, R. Perry, C.K. Ober, E.J. Kramer, M.E. Callow, J.A. Callow, D.A. Fischer, Langmuir 22 (2006) 5075–5086.
[17] E.H. Sohn, J. Kim, B.G. Kim, J.I. Kang, J.S. Chung, J. Ahn, J. Yoon, J.C. Lee, Colloids Surf. B: Biointerfaces 77 (2010) 191–199.
[18] C. Satriano, G.M.L. Messina, S. Carnazza, S. Guglielmino, G. Marletta, Mater. Sci. Eng. C 26 (2006) 942–946.
[19] L. Bertin, M. Majone, D. Di Gioia, F. Fava, J. Biotechnol. 87 (2001) 161–177.
[20] R. Mundargi, S.A. Patil, T.M. Aminabhavi, Carbohydr. Polym. 69 (2007), 130 141.
[21] I.G. Mandala, E. Bayas, Food Hydrocolloids 18 (2004) 191–201.
[22] H. Makamba, J.H. Kim, K. Lim, N. Park, J.H. Hahn, Electrophoresis 24 (2003) 3607–3619.
[23] J.K. Liu, M.L. Lee, Electrophoresis 27 (2006) 3533–3546.
[24] T. Vilkner, D. Janasek, A. Manz, Anal. Chem. 76 (2004) 3373–3385.
[25] D.C. Duffy, J.C. McDonald, O.J.A. Schueller, G.M. Whitesides, Anal. Chem. 70 (1998) 4974–4984.
[26] D.Q. Xiao, H. Zhang, M. Wirth, Langmuir 18 (2002) 9971–9976.
[27] G.D. Sui, J.Y. Wang, C.C. Lee, W.X. Lu, S.P. Lee, J.V. Leyton, A.M. Wu, H.R. Tseng, Anal. Chem. 78 (2006) 5543–5551.
[28] W. Hellmich, J. Regtmeier, T.T. Duong, R. Ros, D. Anselmetti, A. Ros, Langmuir 21 (2005) 7551–7557.
[29] E. Delamarche, M. Geissler, A. Bernard, H. Wolf, B. Michel, J. Hilborn, C. Donzel, Adv. Mater. 13 (2001) 1164–1167.
[30] V. Barbier, M. Tatoulian, H. Li, F. Arefi-Khonsari, A. Ajdari, P. Tabeling, Langmuir 22 (2006) 5230–5232.
[31] Q.G. He, Z.C. Liu, P.F. Xiao, R.Q. Liang, N.Y. He, Z.H. Lu, Langmuir 19 (2003) 6982–6986.
[32] S.W. Hu, X.Q. Ren, M. Bachman, C.E. Sims, G.P. Li, N. Allbritton, Anal. Chem. 74 (2002) 4117–4123.
[33] S.W. Hu, X.Q. Ren, M. Bachman, C.E. Sims, G.P. Li, N.L. Allbritton, Langmuir 20 (2004) 5569–5574.
[34] Y.S. Shin, K. Cho, S.H. Lim, S. Chung, S.J. Park, C. Chung, D.C. Han, J.K. Chang, J. Micromech. Microeng. 13 (2003) 768–774.
[35] K. Pederson, Water Res. 24 (1990) 239–243.
[36] I. Chang, E.S. Gilbert, N. Eliashberg, J.D. Keasling, Microbiology 149 (2003) 2859–2871.
[37] S.M. Hunt, E.M. Werner, B. Huang, M.A. Hamilton, P.S. Stewart, Appl. Environ. Microbiol. 70 (2004) 7418–7425.